

5

Turbulent mixing and chemical reactions

The purpose of this chapter is to give an introduction to problems faced by engineers wanting to use CFD for detailed modelling of turbulent reactive flows. After reading this chapter you should be able to describe the physical process of turbulent mixing and know why this can have an effect on the outcome of chemical reactions, e.g. combustion. The problem arises when the grid and time resolution is not sufficient to resolve the concentration and the average concentration in the cells is a poor estimation of the actual concentration as shown in Figure 5.1. The local concentration changes fast, and we need models that can predict the space- and time-average reaction rate in each computational cell.

The average concentration in a computational cell can be used to describe macromixing (large-scale mixing) in the reactor and is relatively straightforward to model. The concentration fluctuations, on the other hand, can be used to describe micromixing (small-scale mixing on the molecular level). To quantify micromixing, the variance of the concentration fluctuations is used. Chemical reactions can take place only at the smallest scales of the flow, after micromixing has occurred, because reactions occur only as molecules meet and interact. An expression for the instantaneous rate of chemical reactions is often known for homogeneous mixtures. However, the average rate of chemical reactions in a reactor subject to mixing will depend also on the rate of micromixing.

In modelling fast reactions it is not sufficient to know the time-average concentration since at a specific position only one of the reactants may be present for some fraction of the time and no reaction will occur. The models for the average reaction rate make use both of the average concentrations and of the variance. The time average alone will not tell us whether both reactants were present simultaneously. A large variance tells us that the instantaneous concentration is far from the average and the probability that both reactants are present is low, whereas a small variance tells us that the concentrations of both reactants are close to the average and there is a high probability that both are present simultaneously. Hence, it is of great importance to understand that the average and variance represent macromixing and micromixing on the largest and smallest scales of the flow, respectively. In this chapter we will present the tools required to describe the flow and simulate concentration variations using probability density functions (PDFs), and use them to calculate average reaction rates.

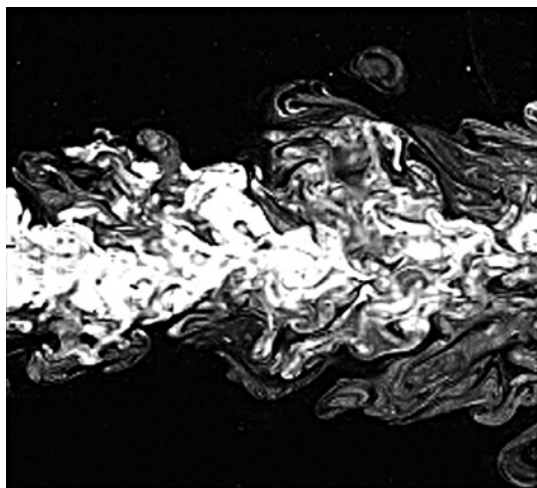


Figure 5.1 The instantaneous concentration field in a turbulent flow.

5.1 Introduction

Mathematical modelling of turbulent reactive flows is of great interest for a wide variety of applications in chemical-process engineering and combustion engineering. In chemical engineering a reactor serves, among other things, to mix species in an effort to obtain a desired reaction. It has been realized that the way in which reactants are mixed can actually be very important for the outcome of mixing-sensitive reactions. Only recently have efficient and reliable mathematical models that are able to incorporate these effects of mixing been developed. More exactly, these models are able to describe the initial mixing between fluids accurately, which can be of crucial importance. In this regard CFD is an invaluable tool since the whole reactor, including the injection, can be discretized and modelled in great detail.

Nonetheless, the process industry has been rather slow at taking advantage of this fact, and highly advanced CFD models are not very often used in the development of chemical reactors. In mechanical engineering there has always been a greater incentive for development, since there is here a major economical benefit to be derived from even the slightest improvement of a turbulent combustion engine. There are also a wider range of utilities (e.g. diesel engines, spark-ignition engines, furnaces, gas turbines), more severe reacting conditions and generally more stringent regulations for pollution, forcing improvements of existing tools. Of interest to the engineer is the fact that the bulk of the mathematical models derived for non-premixed turbulent gaseous combustion are equally valid for the liquid flows more commonly encountered in the process industry.

However, the relative success of a CFD analysis will be completely reliant on the accuracy of the mathematical model used for describing the underlying physics. Furthermore, as will be shown in this section, there will always have to be a certain level of modelling, since the physics of turbulent reactive flows is too complex to be fully resolved from first principles. In general there will have to be a trade-off between level

of description and computational efficiency, in a hierarchy of models. In fact, the more of the flow is modelled, the less expensive the computations will be.

The highest-level mathematical descriptions of a turbulent reactive flow use only first principles and no modelling, i.e. direct numerical simulation (DNS). However, this approach is completely impractical for all industrial applications due to the enormous computational cost. The next-level large-eddy simulation (LES) models only the smallest scales of the flow (molecular mixing and chemical reactions), whereas the lowest level computes only statistical properties. Except for the highest level, the calculations are in general still not accurate enough to make experiments superfluous. However, for many systems there are models available that can give at least reasonably reliable predictions, completely without the aid of experiments. Still, it is our firm belief that the optimal design of a chemical reactor or combustion unit will be achieved through a balanced unification of experience, experiments and simulations.

The most common application area for reactive-mixing models is in turbulent combustion. The problem of mixing and reaction is exactly the same in combustion as in chemical reactors, but one must also take into account the sometimes large density and temperature fluctuations in combustion. This complicates the mathematical description and sometimes requires models that are used only for combustion. In combustion it is also common for the species to be premixed, whereupon reactions start only after ignition. This exact problem is not encountered in chemical reactors. In what follows we will assume that the reactants are initially separated (non-premixed), that the heat release from the reactions is small (so that the temperature fluctuations will be negligible) and that the density is constant. We will address only pure reaction-and-mixing problems, i.e. problems in which turbulent mixing has a direct effect on the outcome of chemical reactions. This is commonly referred to as the turbulence-chemistry effect. Hence we will not discuss more classical reaction problems involving more than one phase, e.g. packed beds, monoliths, reactive distillation etc.

5.2 Problem description

Danckwerts (in 1958) was the first chemical engineer to study the influence of mixing on the evolution of chemical reactions. Danckwerts established that for some reactions the way in which species were mixed could severely affect the product selectivity. This was in sharp contrast to reactor models routinely used by chemical engineers that neglected the effects of mixing, e.g. ideal batch, perfectly mixed continuously stirred tank reactors or plug flow. However, far from all reactions are mixing-sensitive, and these reactor models still serve a purpose in the process industry. In general, if chemical reactions are slow, mixing has no influence on the mean rate of reaction and the 1D ideal reactor models suffice. This follows since the reactants will be well mixed on the smallest scales (micromixing will be complete) before substantial reactions can occur. The only real problem is then that of how to obtain an accurate rate expression for the chemistry. When the typical time required for mixing is of the same order as, or longer than, the typical time required for reactions, mixing models must be introduced to describe the

physics and to get realistic results for selectivity calculations. Furthermore, fast reactions depend very much on how reactants are mixed and on the geometry of the reactor. CFD simulations are then necessary for sufficient accuracy.

To illustrate the main problem in modelling of reactive flows, consider a single irreversible reaction leading to some products:



The chemical reaction rate is now assumed to be second order with rate constant k_1 . Mathematically this can be represented as

$$S_A = S_B = -k_1 C_A C_B. \quad (5.2)$$

In statistical modelling of turbulent reactive flows one is interested in the average, not the instantaneous, rate of the chemical reactions. For this reason it is common to introduce Reynolds decomposition (see Section 4.2.3) of the instantaneous concentration into its mean and fluctuating parts. Representing the average with angle brackets and fluctuation about the average with primes, the instantaneous concentration can be decomposed as $C_\alpha = \langle C_\alpha \rangle + C'_\alpha$. Inserting for this in Eq. (5.2) and taking the average leads to the following expression for the average reaction rate:

$$\langle S_A \rangle = \langle S_B \rangle = -\langle k_1 C_A C_B \rangle = -k_1 (\langle C_A \rangle \langle C_B \rangle + \langle C'_A C'_B \rangle). \quad (5.3)$$

The time-averaged concentrations $\langle C_A \rangle$ and $\langle C_B \rangle$ are easily available in the simulations, but the covariance of the fluctuating components $\langle C'_A C'_B \rangle$ is the major problem in modelling of turbulent reactive flows. Note that for slow reactions that term will be zero, since there will be no fluctuations left when the reactions start to occur, i.e. micromixing will be complete and the mixture will be homogeneous. Hence for slow reactions there is no turbulence-chemistry effect and Eq. (5.3) will be closed. Since fast chemical reactions occur during the early stages of mixing, there will during the course of reactions be large local concentration fluctuations, as illustrated in Figure 5.2. In Figure 5.2 there are large areas containing only A or only B, where no reactions can occur. The reactions occur only when A and B are present simultaneously, and here the term $\langle C'_A C'_B \rangle$ can be significant.

The term $\langle C'_A C'_B \rangle$ is the reactive-mixing analogy to the Reynolds stress $u_i u_j$. We know from Chapter 4 that the convective Reynolds stress usually can be modelled as a diffusion process, due to the chaotic nature of turbulence. In other words, diffusion is used to model convection. Unfortunately, there is no such analogy known for $\langle C'_A C'_B \rangle$. In fact, it has been proven that in general it is not possible to model $\langle C'_A C'_B \rangle$ using merely the average (macroscale) concentrations $\langle C_A \rangle$ and $\langle C_B \rangle$, their gradients or the rate of mixing, which complicates matters significantly. In other words, it has been realized that, for sufficient accuracy in modelling of chemical reactions, greater levels of complexity are necessary than for pure flow computations. Since the complexity is so high, we will not go into great detail or give a complete review of the current state of the art. Instead, we will first discuss the nature of reactive mixing and then discuss the simplest models that can be incorporated into commercial CFD software.

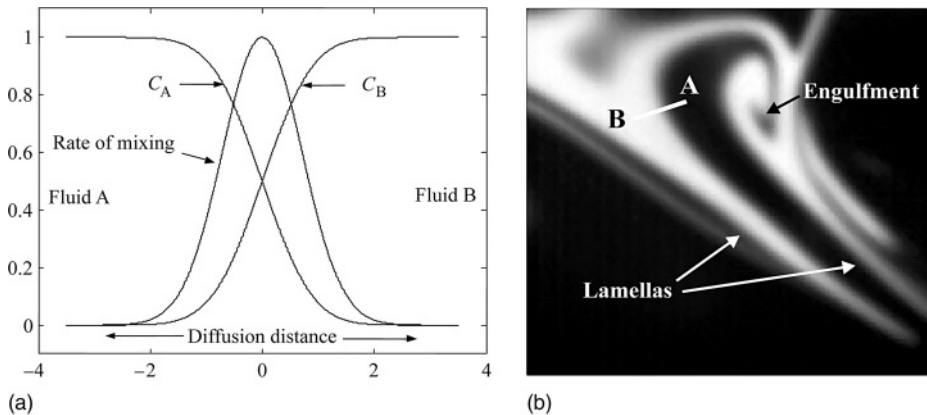


Figure 5.2 Mixing across an interface. (a) Concentration profiles across an interface between fluids A and B at the position shown with the thick white line in (b). (b) An instantaneous image of mixing between A and B in a turbulent flow field. The image is $2 \text{ mm} \times 2 \text{ mm}$. $\eta_B \approx 3 \text{ } \mu\text{m}$ and $\eta_K \approx 150 \text{ } \mu\text{m}$ (see Section 5.4), which gives a diffusion distance of about η_K .

5.3 The nature of turbulent mixing

Mixing is the process that acts on initially separated (non-premixed) fluids, resulting in a final homogeneous mixture. When white milk is poured into a cup of black coffee, the result will eventually be a new homogeneous, brown mixture. If the cup is initially stirred with a spoon the mixing time can be seconds. However, without stirring the milk can take several minutes to blend in. In other words, stirring can significantly increase the rate of mixing.

The nature of reactive mixing is quite easily understood once you realize that it is all about getting molecules to meet and interact. The most efficient way to achieve this is generally through agitation (stirred tanks) or simply by creating a high enough velocity to obtain turbulence (pipe flow). Either way, the main objective is to achieve turbulence. First of all the mean flow and the largest scales of turbulence lead to efficient macromixing, i.e. the reacting components can be quickly distributed over the whole reactor geometry. Hence, macromixing is mixing on the largest scales of the reactor. However, chemical reactions occur at the smallest scales of the flow where molecules meet and diffusion is important. In fluid mixing, turbulence is the process that acts on a fluid element, causing continuous deformation and stretching (to reduce the size of fluid elements) followed by engulfment, which occurs at the very smallest scales and significantly increases the interface area between the fluid element and the bulk. At the smallest scales the reacting components from different fluid elements diffuse into contact and thus reaction can occur.

Understanding what happens at the interfacial area between mixtures is thus of great importance. It is known from experiments that fluid elements in turbulent flows align in layers of lamellas where the concentrations across an interface can be well approximated mathematically with an error function. Figure 5.2(b) shows an instantaneous snap-shot

of binary mixing between fluids A and B in a turbulent flow field. The size of the measured volume corresponds to a computational cell in CFD, and it is evident that the average concentration in a computational cell will give a poor description of the concentration during mixing and fast chemical reactions. The theoretical concentrations and mixing rate (scalar dissipation rate) across an interface are presented in Figure 5.2(a) with error functions. At the smallest scales in Figure 5.2(a) only diffusion is important for the mixing process. Turbulence quickly increases the interfacial area between fluid elements and thus reduces the required diffusion distance, so that the required diffusion time will be small. If turbulence is intense, diffusion will limit the rate of mixing, and vice versa if the intensity is too low.

It is of great importance to estimate whether mixing can be a rate-limiting step in the process. The mixing time must then be compared with a timescale for reaction. A quantity that compares the timescale of chemical reactions with the timescale of mixing is the Damköhler number (Da):

$$Da = \frac{\text{Typical time required for mixing}}{\text{Typical time required for chemical reactions}}. \quad (5.4)$$

The time for mixing is described in the following equation and the typical time for chemical reactions can be estimated with C_α as the concentration of the limiting reactant:

$$\tau = \frac{C_\alpha}{r} = \frac{C_\alpha}{kC_\alpha C_\beta} = \frac{1}{kC_\beta}.$$

There are three possible outcomes from analysis of the Damköhler number:

- (1) $Da \ll 1$. Reactions are slow compared with the rate of mixing. In other words, the reactor will have a homogeneous mixture (no segregation) before any substantial reaction can take place. The concentrations in the computational cells are sufficiently well described by the average concentration in the cell. For this scenario standard chemical-reactor models such as the plug-flow reactor or the continuously stirred tank reactor may suffice.
- (2) $Da \gg 1$. Reactions are very fast or instantaneous, e.g. acid–base reactions, ion–ion reactions and some gaseous combustion reactions. This problem often benefits from CFD modelling since the common reactor models are inapplicable. Furthermore, since the reactions are instantaneous, it can be shown that studying the evolution of a conserved scalar suffices to get a complete description of the problem (see Section 5.5.2). A conserved scalar is an inert, or passive, tracer, and it is much easier to study the conserved scalar than reactive species because the (usually nonlinear) chemical reaction rate need not be modelled.
- (3) $Da \approx 1$. The timescales for reaction and mixing are of the same order of magnitude. This scenario is by far the most difficult and requires complex modelling for accurate predictions of the mean chemical reaction rates. The case cannot be described by traditional reactor models. Engineers have commonly solved this problem by using Lagrangian micromixing models. However, these models neglect inhomogeneities and reactor geometry.

In modelling of cases (2) and (3) the most successful CFD models calculate first the mixing of a conserved scalar to predict the intensity of segregation of the mixture (the state of mixedness). This information can further be used to obtain closures for the mean chemical reaction rate. When reading Section 5.4 it is important to remember that, even though we are addressing only a conserved scalar, prediction of the mean chemical reaction rate is the overall main objective.

5.4 Mixing of a conserved scalar

To estimate the Damköhler number it is necessary to get an idea of the relevant length scales and timescales for mixing and reactions in the system concerned. These scales can be found from simulations of the flow field (the turbulence variables k and ε are usually sufficient) with some model taken from Section 4.2, or from experiments. It is, for example, possible to measure the pressure drop over a chemical reactor and from this estimate the corresponding average rate of energy dissipation. It is also necessary to gain knowledge of the rate expressions for the chemical reactions (like Eq. (5.2)) and the diffusivity of the reacting species. The smallest length scales and timescales that are important for chemical reactions are generally not the same as for the flow (see Chapter 4 about the Kolmogorov scales). This follows since the molecular diffusivity of species in liquids is usually much lower than the kinematic viscosity of the fluid. The smallest relevant length scale for reacting flows will be the average distance a molecule diffuses during the Kolmogorov timescale. This scale is characterized by the Batchelor length scale η_B , which is represented as

$$\eta_B = Sc^{-1/2} \eta_K. \quad (5.5)$$

The Schmidt number Sc describes how fast transport of momentum is relative to the transport of molecules ($Sc = \nu/D$). For gases the Schmidt number is approximately unity and the Batchelor scale more or less equals the Kolmogorov scale. For water-like liquids and not-too-large molecules, the Schmidt number is usually close to 1000. The Schmidt number is high for liquids since momentum can be transported by collisions of molecules, whereas molecular diffusion represents the movement of individual molecules.

5.4.1 Mixing timescales

The stages of mixing during which fluid elements are deformed and reduced in size followed by molecular diffusion are referred to in combination as micromixing. The initial step, i.e. deformation and stretching, is referred to as inertial–convective mixing since the fluid elements are merely transported from large eddies to small eddies through convection. The timescale for this process is merely the inverse of the rate of mixing. Hence, modelling of timescales and modelling of mixing rates are equivalent, the timescale used for describing inertial–convective mixing being

$$\tau_{IC} = \theta \frac{k}{\varepsilon}, \quad (5.6)$$

where θ is a constant commonly set to 0.5. There is no Schmidt-number dependence since viscosity and diffusion are not relevant. For gases ($Sc \approx 1$) this single timescale suffices for a complete description of the mixing process.

At scales just below η_K convective and viscous mixing are of the same order of magnitude, whereas diffusion is still too slow to interfere for $Sc \gg 1$. Mixing on this scale is commonly referred to as engulfment or viscous–convective mixing. The timescale for engulfment is often determined by

$$\tau_{VC} = 17.25 \sqrt{\frac{\nu}{\varepsilon}}. \quad (5.7)$$

The final stage of mixing during which all spatial gradients disappear and a homogeneous mixture is obtained occurs near the Batchelor scale. Mixing at this scale is referred to as viscous–diffusive mixing since both viscosity and diffusion are important. The timescale for viscous–diffusive mixing is given as

$$\tau_{VD} = \frac{\tau_{VC}}{0.303 + 17\,050 Sc^{-1}}, \quad (5.8)$$

which is proportional to the viscous–convective timescale, but with a Schmidt-number dependence.

Typical average data for a large stirred-tank reactor with water at room temperature are $k \approx 0.05 \text{ m}^2 \text{ s}^{-2}$ and $\varepsilon \approx 1 \text{ W kg}^{-1}$, giving $\tau_{IC} = 25 \text{ ms}$, $\tau_{VC} = 17 \text{ ms}$ and $\tau_{VD} \approx 1 \text{ ms}$. Only fast reactions in which a noticeable amount has reacted within 1 s need to be modelled using mixing models. The mixing time for the reactor, i.e. the time taken to reach the same concentration in the whole reactor, is of the order of minutes, and the ideal stirred-tank reactor may still be a poor model. The local rate of dissipation around the impeller is an order of magnitude higher than the average, and good mixing for fast reactions can be obtained when the reactants are added in the impeller region and the opposite behaviour is obtained close to the reactor surface.

The characterization of timescales for mixing described in this section is only one of several suggestions that have appeared in the literature. However, all mixing models are similar insofar as one must make use of the same parameters that are available from flow-field computations (ν , k , ε and Sc). The important lesson is that you now have some tools that can be used to get a first understanding of the problem at hand, through describing the reactions as slow, fast or instantaneous compared with mixing. You can, for example, use the knowledge from this section to determine the local rate of mixing in a stirred tank, which is important for finding the optimal position for injection of a reactant. Usually it is most efficient to inject where the rate of mixing is fastest, e.g. in the impeller region.

5.4.2 Probability density functions

In modelling of reactive mixing a very important tool is the probability density function (PDF) of a mixture fraction (a conserved scalar, i.e. a non-reacting species). The mixture fraction $\xi(\mathbf{x}, t)$ is defined for binary mixtures (mixtures with two inlets) as unity for one inlet stream and zero for the other. The name mixture fraction is thus logical since it

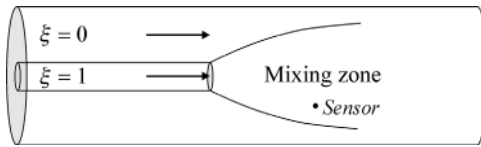


Figure 5.3 Mixing in pipe flow.

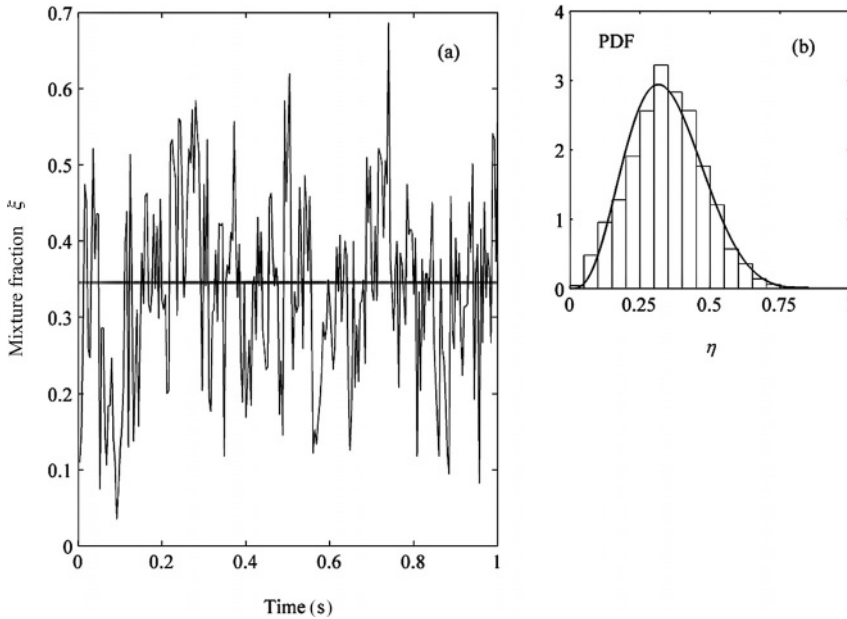


Figure 5.4 Measurements of the mixture fraction at a position in the mixing zone in Figure 5.3. (a) Raw data. (b) Histogram (PDF) of the instantaneous measurements. Here the solid line represents the beta-PDF with mean and variance taken from the experiment. The bars represent the experimental data.

describes how large a fraction of the flow at a certain point has historically come from the injection with a value of unity. Consider an injection in the centre of a turbulent pipe flow (Figure 5.3). This figure shows the instantaneous concentration of the mixture fraction at the injection. If you measure continuously at any (infinitesimally small) point in the pipe, you will obtain a time series of concentrations as shown in Figure 5.4. Figure 5.4(a) shows the raw data with all the characteristics of a chaotic turbulent flow. Like all turbulent measurements, the data will make sense only when some averaging procedure is performed. Figure 5.4(b) shows the histogram, or probability density, of the raw data.

The PDF φ is defined as the probability of measuring a certain concentration η of the tracer:

$$\varphi(\eta)d\eta \equiv \text{probability of } \{\eta \leq \xi \leq \eta + d\eta\}, \quad (5.9)$$

where η is a sample-space variable for ξ . A sample space is the collection of all possible outcomes of an event. A variable used to describe a single event in sample space is a sample-space variable. In mixture-fraction space η is thus the sample-space variable used to describe the real event ξ .

The sample space of the mixture fraction spans from zero to unity, as shown in Figure 5.4(b), since these two extremes represent pure mixtures. A logical effect of mixing is that the mixture fraction cannot take on values outside this range. For a single bin in the histogram of Figure 5.4(b), $d\eta$ is chosen to have the discrete value of 0.05, but for a continuous PDF $d\eta \rightarrow 0$. By definition the integral of the PDF must equal unity:

$$\int_0^1 \varphi(\eta) d\eta = 1. \quad (5.10)$$

For the discrete histogram the integral is defined as the summation over all the bins:

$$\sum_{\text{bins}} \varphi(\eta) d\eta = 1. \quad (5.11)$$

Another way to think of the PDF is that it describes the fraction of time that the mixture fraction spends in the state η , i.e. the fraction of time a certain concentration or mixture fraction is observed.

The PDF contains all single-point information of the mixture fraction. Given the PDF, all mixture fraction moments (mean, variance, skewness etc.) can be found by integration over mixture-fraction space. The mean $\langle \xi \rangle$ and variance σ^2 (second central moment) of the mixture fraction are defined through the PDF as

$$\langle \xi \rangle = \int_0^1 \eta \varphi(\eta) d\eta \quad \text{and} \quad \sigma^2 = \int_0^1 (\eta - \langle \xi \rangle)^2 \varphi(\eta) d\eta. \quad (5.12)$$

It can be seen from Figure 5.4(b) that for this particular PDF the probability of measuring a mixture fraction close to the mean is relatively large. In other words, the variance is small. What happens during mixing is that the variance will gradually decrease until eventually the mixture is homogeneous, the variance will be zero and the PDF can be described by a single delta-function. In Figure 5.5 the evolution of the PDF for mixing in a homogeneous turbulent flow field with a presumed beta-PDF as a model for φ (the mean mixture fraction will be constant and the variance will decrease exponentially in time) is shown. The beta-PDF uses the mean and variance of the mixture fraction to give a continuous distribution. The beta-PDF φ_B is defined as

$$\varphi_B(\eta; a, b) = \frac{\eta^{a-1} (1 - \eta)^{b-1}}{B(a, b)}, \quad (5.13)$$

A semicolon is used to denote that η is a sample-space variable, whereas a and b are fixed parameters. The coefficients are easily calculated from the average ξ and the variance σ^2 as

$$a = \langle \xi \rangle \left[\frac{\langle \xi \rangle (1 - \langle \xi \rangle)}{\sigma^2} - 1 \right], \quad b = \frac{1 - \langle \xi \rangle}{\langle \xi \rangle} a \quad (5.14)$$

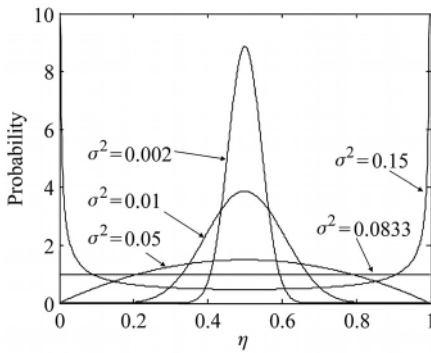


Figure 5.5 Mixing in homogeneous turbulence as described with the beta-PDF. $\langle \xi \rangle = 0.5$.

and $B(a, b)$ is given by the gamma-function Γ that can be found in most mathematical tables:

$$B(a, b) = \int_0^1 s^{a-1} (1-s)^{b-1} ds = \frac{\Gamma(a) \Gamma(b)}{\Gamma(a+b)}. \quad (5.15)$$

It can be seen from Figure 5.5 that the PDF from the experiment nearly coincides with the presumed beta-PDF. This simple observation (that the shape of the beta-PDF nearly resembles the experimentally observed shape of the mixture-fraction PDF) has been used extensively in many closures for reactive flows. There is still no theoretical justification for using the beta-PDF, though, but it is known to give a very good description of mixing in homogeneous flows. For inhomogeneous flows the accuracy is known to be worse, and it is not necessarily a good approximation. Inhomogeneous flows have significant spatial gradients of the calculated properties. In other words, convection and diffusion cannot be neglected in the governing equations. It is generally possible to obtain homogeneous flows only in laboratories or in numerical experiments (DNS).

Nonetheless, the presumed beta-PDF is the most extensively used PDF even for inhomogeneous flows. The advantage with the beta-PDF is that it is a function only of the average ξ and the variance σ^2 , and only ξ and σ^2 must be simulated in order to obtain the PDF. Note that the beta-PDF can be accurate only when there are two distinct inlet streams. Consider a case of three separate inlets. One stream has pure tracer ($\xi = 1$), one stream has only water ($\xi = 0$) and the last is a diluted-tracer stream (e.g. a recirculation stream with $\xi = \frac{1}{2}$). The initial PDF will then exhibit three distinct peaks at 0, $\frac{1}{2}$ and 1. The beta-PDF can initially only peak at 0 and 1, and is thus unable to reproduce the experimentally observed PDF. To be able to compute PDFs with multiple peaks, one will have to use more than two moments of the mixture fraction or more than just the one single-mixture fraction. A discussion of this difficult topic is beyond the scope of this book, though.

The presumed beta-PDF has no physical foundation; it is only a convenient description of the mixing, and there are other suggestions for the presumed PDF. The most common are a clipped Gaussian or some ensemble of delta-functions. A presumed PDF that can

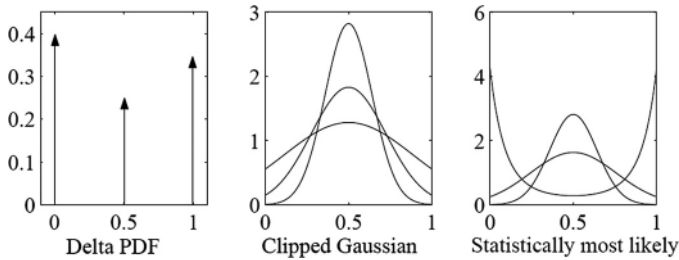


Figure 5.6 Some presumed PDFs. The three realizations of the Gaussian and the statistically most likely PDFs have the same moments ($\langle \xi \rangle = 0.5$, $\langle \xi'^2 \rangle = 0.15, 0.05, 0.02$). The delta PDF has $\langle \xi \rangle = 0.48$ and $\langle \xi'^2 \rangle = 0.19$.

take any number of moments from the mixture fraction is the statistically most likely (SML) PDF [14]. Owing to the possibility of including more moments, the SML PDF can accurately describe even strongly inhomogeneous flows. However, the parameters of the SML PDF have to be found from iterations and thus more computational power is required than for the beta-PDF. Also, the closures for higher moments of the mixture fraction are not nearly as well investigated as those for the mean and the variance. In Figure 5.6 some realizations of the different presumed PDFs are shown.

5.4.3 Modelling of turbulent mixing

The mixture-fraction PDF involves just the first two moments of the mixture fraction, and these moments must be predicted in the mixing model. Transport equations for any moment follow quite simply from manipulations of the transport equation for the instantaneous mixture fraction:

$$\frac{\partial \xi}{\partial t} + U_j \frac{\partial \xi}{\partial x_j} = \frac{\partial}{\partial x_j} \left(D \frac{\partial \xi}{\partial x_j} \right). \quad (5.16)$$

In the simplest case the mixture fraction is merely a normalized concentration and this equation is identical to Eq. (2.1) without the reaction and source terms. We know that Eq. (5.16) can in general not be solved directly, since U_i is unknown, and requires an extremely dense grid resolution for accurate solutions (DNS, see Section 4.2.1). Reynolds decomposition of the velocity and mixture fraction ($U_i = \langle U_i \rangle + u_i$ and $\xi = \langle \xi \rangle + \xi'$) followed by Reynolds averaging of the resulting equation leads to an equation that is more easily solved, but that contains information only on the average mixture fraction:

$$\frac{\partial \langle \xi \rangle}{\partial t} + \langle U_j \rangle \frac{\partial \langle \xi \rangle}{\partial x_j} = - \frac{\partial}{\partial x_j} \left(\langle u_j \xi' \rangle - D \frac{\partial \langle \xi \rangle}{\partial x_j} \right). \quad (5.17)$$

In Eq. (5.17) the first term is accumulation, the second is convection by the mean flow, the third is turbulent transport and the last is molecular diffusion, which usually can be neglected since D is small. The flux $\langle u_j \xi' \rangle$ is unclosed and requires modelling (e.g. Eq. (5.24)). The mean mixture fraction is represented by a thick line in Figure 5.4(a). All detailed information is lost upon this averaging. The mean mixture fraction

describes macromixing and gives information about the largest scales of the reactor. It is, however, useless for predicting the level of mixing on the smallest scales (micromixing) which are important for fast or instantaneous chemical reactions.

Micromixing is often described by the mixture-fraction variance which was previously defined through the PDF in Eq. (5.12). The variance can be interpreted as a local average departure from homogeneity, and it is thus a local measure of segregation. With reference to Figure 5.4(a), the variance can be understood as the intensity of the fluctuations around the mean. Strong fluctuations mean a large variance (high degree of segregation). The maximum variance that can be achieved occurs when all measurements are either zero or unity (the existence of no intermediate values means that no mixing has occurred). The value of the variance will then equal $\sigma_{\max}^2 = \langle \xi \rangle (1 - \langle \xi \rangle)$, which is often used for normalization. The resulting normalized variance is termed the intensity of segregation I_S :

$$I_S = \frac{\sigma^2}{\langle \xi \rangle (1 - \langle \xi \rangle)}. \quad (5.18)$$

The intensity of segregation always starts with the value of unity under non-premixed initial conditions.

A transport equation for σ^2 can be found by multiplying Eq. (5.16) by 2ξ , Reynolds decomposing U_i and ξ , and then taking the Reynolds average of the whole equation:

$$\frac{\partial \sigma^2}{\partial t} + \langle U_j \rangle \frac{\partial \sigma^2}{\partial x_j} = - \frac{\partial}{\partial x_j} \left(\langle u_j \xi'^2 \rangle - D \frac{\partial \sigma^2}{\partial x_j} \right) - 2 \langle u_j \xi' \rangle \frac{\partial \langle \xi \rangle}{\partial x_j} - 2D \left\langle \frac{\partial \xi'}{\partial x_j} \frac{\partial \xi'}{\partial x_j} \right\rangle. \quad (5.19)$$

To derive Eq. (5.19) we have also used Eq. (5.17) and the following identity:

$$\xi \frac{\partial \xi}{\partial x_i} = \frac{1}{2} \frac{\partial \xi^2}{\partial x_i}. \quad (5.20)$$

The left-hand side of Eq. (5.19) is accumulation and convection. On the right-hand side the first term is turbulent transport and molecular diffusion, the second is production due to interaction between a flux and the gradient of the mean mixture fraction, and the last term is twice the mean scalar dissipation rate, which we henceforth denote $\langle N \rangle$ (see Eq. (5.32)). The mean scalar dissipation rate is the scalar analogue of the mean energy-dissipation rate ε and is always positive. Physically, this term describes how fast the mixture-fraction variance is disappearing due to diffusion at the smallest scales.

Note that, even though Eq. (5.19) is an exact equation for the mixture-fraction variance, problems could arise from its solution. The intensity of segregation cannot, by definition, be larger than unity. However, with the solution of Eq. (5.19) there is nothing to ensure that this limit is respected. Problems can arise due to the production term and the closure for the first-order flux $\langle u_j \xi' \rangle$ (see Eq. (5.24)). There is a nice solution to this problem, though. Instead of solving for Eq. (5.19) directly, you can solve for the equivalent

second raw moment σ_R^2 . The second raw moment is defined as the second moment around zero:

$$\sigma_R^2 = \langle \xi^2 \rangle = \int_0^1 \eta^2 \varphi(\eta) d\eta. \quad (5.21)$$

A transport equation for σ_R^2 can be found by exactly the same procedure as for Eq. (5.19), but without decomposition of ξ . The resulting equation reads

$$\frac{\partial \sigma_R^2}{\partial t} + \langle U_j \rangle \frac{\partial \sigma_R^2}{\partial x_j} = - \frac{\partial}{\partial x_j} \left(\langle u_j \xi^2 \rangle - D \frac{\partial \sigma_R^2}{\partial x_j} \right) - 2D \left\langle \frac{\partial \xi}{\partial x_j} \frac{\partial \xi}{\partial x_j} \right\rangle. \quad (5.22)$$

On implementing Eq. (5.22) instead of Eq. (5.19) you will not get any problems of realizability (unphysical results) since there is no production involved. It also ensures that the intensity of segregation initially starts out as exactly unity. To obtain the central variance from the raw moment, simply apply the following formula:

$$\sigma^2 = \sigma_R^2 - \langle \xi \rangle^2. \quad (5.23)$$

In Eqs. (5.17), (5.19) and (5.22) closure is required for $\langle u_j \xi' \rangle$, $\langle u_j \xi'^2 \rangle$, $\langle u_j \xi^2 \rangle$ and $\langle N \rangle$, so these terms will now be discussed further. The first three terms are fluxes, and are thus required to conserve the mean upon transport (the spatial derivative of the flux is convection, which is conservative). The only way to achieve this is through gradient-diffusion models or by deriving completely new transport equations for the fluxes (that again will contain unknown terms requiring closure). In engineering only the first option is usually employed. The closures for the fluxes thus become

$$\langle u_j \xi' \rangle = -D_T \frac{\partial \langle \xi \rangle}{\partial x_j}, \quad (5.24)$$

$$\langle u_j \xi'^2 \rangle = -D_T \frac{\partial \sigma^2}{\partial x_j} \quad (5.25)$$

$$\langle u_j \xi^2 \rangle = -D_T \frac{\partial \sigma_R^2}{\partial x_j}. \quad (5.26)$$

Here D_T is the turbulent diffusivity, which is commonly calculated as

$$D_T = \frac{\nu_T}{Sc_T}. \quad (5.27)$$

The exact form of D_T will depend on the turbulence model used for ν_T (see Chapter 4). The turbulence Schmidt number Sc_T is known to vary between approximately 0.5 and 1.5, but is most commonly set to 0.7. The near-unity value of Sc_T means that turbulent transport (macromixing) of momentum and species is almost identical for most flows. Note that the gradient closures (Eqs. (5.24) – (5.26)) are closely related to the Boussinesq hypothesis used for modelling of the Reynolds stresses discussed in Section 4.2.4.

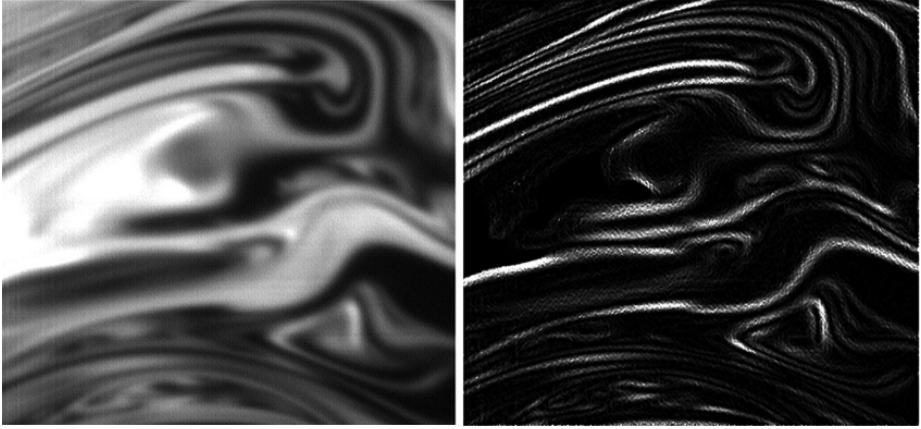


Figure 5.7 Concentration fluctuations (left) and scalar dissipation (right).

The closed models for the average mixture fraction, the variance and the raw variance are then obtained as

$$\frac{\partial \langle \xi \rangle}{\partial t} + \langle U_j \rangle \frac{\partial \langle \xi \rangle}{\partial x_j} = \frac{\partial}{\partial x_j} \left((D + D_T) \frac{\partial \langle \xi \rangle}{\partial x_j} \right), \quad (5.28)$$

$$\frac{\partial \sigma^2}{\partial t} + \langle U_j \rangle \frac{\partial \sigma^2}{\partial x_j} = \frac{\partial}{\partial x_j} \left((D + D_T) \frac{\partial \sigma^2}{\partial x_j} \right) + 2D_T \frac{\partial \langle \xi \rangle}{\partial x_j} \frac{\partial \langle \xi \rangle}{\partial x_j} - 2D \left\langle \frac{\partial \xi'}{\partial x_j} \frac{\partial \xi'}{\partial x_j} \right\rangle, \quad (5.29)$$

$$\frac{\partial \sigma_R^2}{\partial t} + \langle U_j \rangle \frac{\partial \sigma_R^2}{\partial x_j} = \frac{\partial}{\partial x_j} \left((D + D_T) \frac{\partial \sigma_R^2}{\partial x_j} \right) - 2D \left\langle \frac{\partial \xi}{\partial x_j} \frac{\partial \xi}{\partial x_j} \right\rangle. \quad (5.30)$$

The most important term to close in turbulent mixing is the mean scalar dissipation rate. In Figure 5.2(a) we have already shown a realization of the instantaneous scalar dissipation rate. When the instantaneous scalar dissipation is sampled at the same point over a sufficiently long period of time, we obtain the mean. Note that the mean scalar dissipation rate is the only term, besides transport, that requires closure for turbulent-mixing problems. The scalar dissipation rate describes how fast the final small-scale mixing occurs, or how fast we are obtaining a homogeneous mixture. In Figure 5.2 we have shown the interface between two fluids undergoing mixing. The scalar dissipation rate is defined as the molecular diffusivity times the square of the gradient of the scalar:

$$N = D \frac{\partial \xi}{\partial x_j} \frac{\partial \xi}{\partial x_j}. \quad (5.31)$$

Since the magnitude of the scalar gradient is largest at the centre of the interface, this is where mixing will be fastest. Figure 5.7 shows that the interfaces can be very narrow in high-Schmidt-number liquids, which is why mixing is often referred to as an intermittent phenomenon. By this we mean that a very small part of the total volume of a reactor actually contributes to the final micromixing. Since mixing is fastest at the centre of an

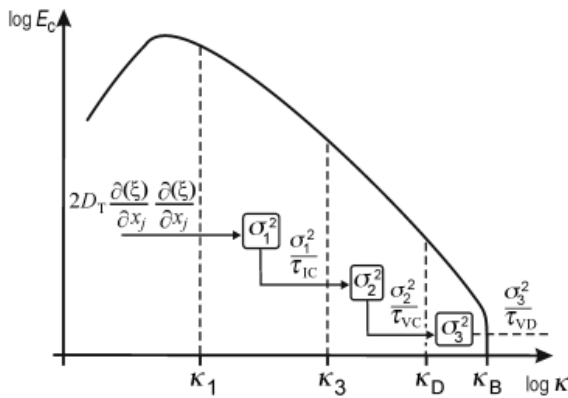


Figure 5.8 The variance cascade in the TMM model.

interface, this is also where the rate of fast chemical reactions (mixing controlled) will peak.

The scalar dissipation rate is more difficult to close for liquids than gases since there is a large separation of scales and any one of inertial–convective, viscous–convective and viscous–diffusive mixing can be rate limiting (see Section 5.4.1). The simplest closures for $\langle N \rangle$ employ a mixing-frequency closure

$$\langle N \rangle = \frac{\sigma^2}{2\tau}, \quad (5.32)$$

where τ is usually calculated as the inertial–convective timescales defined in Eq. (5.6). (Any of the other timescales can still be employed, though.) If this method for predicting $\langle N \rangle$ is too crude, it is possible to obtain higher accuracy through deriving an exact transport equation for $\langle N \rangle$. In practice this is rarely justified, though.

To further complicate modelling of $\langle N \rangle$, the scalar is injected on an inertial scale that usually differs from the largest scales of the flow. Consider again injection at the centre of a turbulent pipe flow (see Figure 5.3). The injected scalar enters the pipe with eddies whose sizes are determined by the radius of the injection pipe. This pipe is, however, much smaller than the radius of the outer pipe, which determines the largest eddies in the main flow. Consequently, close to the injection there will be a transitional region where variance is produced and the largest scale of mixing approaches that of the main flow. To be able to describe this transitional region, a dynamical multi-scale model must be employed. Such a model has been described in detail by Fox [15]. A more intuitive model denoted the turbulent mixer model (TMM) has been described by Baldyga [14] and is presented here. The TMM assumes that the local value of σ^2 can be divided into three parts according to the scales of segregation, namely inertial–convective (σ_1^2), viscous–convective (σ_2^2) and viscous–diffusive (σ_3^2):

$$\sigma^2 = \sigma_1^2 + \sigma_2^2 + \sigma_3^2. \quad (5.33)$$

Further, it is assumed that variance is produced on the macrolevel and dissipated to the smaller scales in a cascade as shown in Figure 5.8. Hence dissipation of σ_1^2 leads to

Table 5.1 Constants in the turbulent mixer model

α	P_α	D_α
1	$2D_T \frac{\partial \langle \xi \rangle}{\partial x_j} \frac{\partial \langle \xi \rangle}{\partial x_j}$	$\frac{\sigma_1^2}{\tau_{IC}}$
2	$\frac{\sigma_1^2}{\tau_{IC}}$	$\frac{\sigma_2^2}{\tau_{VC}}$
3	$\frac{\sigma_2^2}{\tau_{VC}}$	$\frac{\sigma_3^2}{\tau_{VD}}$

production of σ_2^2 and dissipation of σ_2^2 leads to production of σ_3^2 . Dissipation of σ_3^2 , on the other hand, leads to complete mixing. The transport equations for all variances are given as

$$\frac{\partial \sigma_\alpha^2}{\partial t} + \langle U_j \rangle \frac{\partial \sigma_\alpha^2}{\partial x_j} = \frac{\partial}{\partial x_j} \left[(D + D_T) \frac{\partial \sigma_\alpha^2}{\partial x_j} \right] + P_\alpha - D_\alpha \quad \text{for } \alpha = 1, 2, 3 \quad (5.34)$$

and the production P_α and dissipation D_α terms are given in Table 5.1. The molecular-diffusion term in Eq. (5.34) is usually negligible since in general $D_T \gg D$.

The first three terms of Eq. (5.34) account merely for accumulation and transport. The difficult term here is the sink term for the variance, i.e. the scalar dissipation. In the TMM model it is set as the variance divided by the relevant time for each scale.

By summation of the three transport equations and subtraction of Eq. (5.19) we find that the mean scalar dissipation rate is given indirectly as

$$\langle N \rangle = \frac{\sigma_3^2}{2\tau_{VD}}. \quad (5.35)$$

The variance describes the concentration fluctuations in time and at the inlets. With constant concentration all central variances have initial values of zero.

Direct implementations of the TMM will usually lead to realizability problems due to the production term P_1 . As discussed before, the solution to this problem is to use raw, instead of central, moments for the inertial-convective variance σ_1^2 . For the small-scale variances (σ_2^2 and σ_3^2) there will be no problems of realizability, since the production here does not include spatial gradients. Hence they are not subject to discretization errors. To be able to use the TMM for raw moments, simply omit P_1 and set the appropriate initial conditions ($\sigma_{R1}^2 = 1$, where $\langle \xi \rangle = 1$ according to Eq. (5.21), but still with $\sigma_2^2 = \sigma_3^2 = 0$). The dissipation term D_1 must still contain the central variance, now expressed as $\sigma_1^2 = \sigma_{R1}^2 - \langle \xi \rangle^2$. The true raw moment can be recovered as

$$\sigma_R^2 = \sigma_{R1}^2 + \sigma_2^2 + \sigma_3^2 \quad (5.36)$$

and the central moment through Eq. (5.23).

In this section we have discussed only pure mixing. By solving the equations above, we obtain the local mean mixture fraction and variance. The intention has been to obtain a tool for predicting the turbulence-chemistry effect in order to be able to predict the average rate of chemical reactions in each computational cell. In the next section we will discuss how the modelling of a conserved scalar is used in reference to this.

5.5 Modelling of chemical reactions

The modelling hierarchy for reactive flows closely resembles that of pure flows (see Chapter 4). In general you have to give up information in return for computational efficiency. In this regard it is important to understand what information you are giving up and how this can be modelled through simplified relations. As for turbulence modelling the word ‘simplified’ is actually very misleading. The problem is not easier than direct numerical simulation (DNS) of the governing equations. However, DNS is possible only for simple geometries and low Reynolds numbers. Hence, DNS is not an option for chemical reactors and will most likely remain just a research tool in the foreseeable future.

The instantaneous equation for reacting species that is solved in DNS consists of standard accumulation, convection, diffusion and reaction terms:

$$\frac{\partial C_\alpha}{\partial t} + U_j \frac{\partial C_\alpha}{\partial x_j} = \frac{\partial}{\partial x_j} \left(D \frac{\partial C_\alpha}{\partial x_j} \right) + S_\alpha(\mathbf{C}). \quad (5.37)$$

Here \mathbf{C} denotes a vector of all the reacting species in the flow, meaning that the source term for species α , S_α , could depend on any of the other existing species. Since Eq. (5.37) can be solved only for simple geometries with extremely dense meshes (DNS), we must introduce some sort of averaging. Here we consider only Reynolds averaging.

Consider again the reaction described in Eq. (5.1). For a reaction rate $r = kC_A C_B$ the characteristic chemical-reaction timescale can now be given as either $\tau_R = \text{minimum of } 1/(k_1 C_A) \text{ and } 1/(k_1 C_B)$ or $\tau_R = 1/(k_1 C_A + k_1 C_B)$, where the concentrations are defined at the inlets. (Note that, since this is only an approximate timescale, the definitions are not strict.) This timescale should now be used to predict the Damköhler number to see which scenario of Section 5.3 is relevant.

5.5.1 $Da \ll 1$

If the Damköhler number is small there is no problem, since there is sufficient time for local mixing and the covariance term in Eq. (5.3) will be zero. The reaction rate can be expressed merely through the mean concentrations that are already known. The reaction described in Eqs. (5.1)–(5.3) can now easily be closed by neglecting the covariance in Eq. (5.3), and we obtain

$$S_A = -k_1 C_A C_B. \quad (5.38)$$

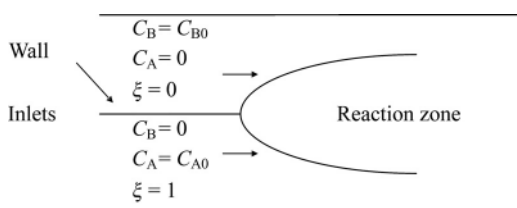


Figure 5.9 A reactive-mixing layer. The reacting species are initially separated by a wall.

The concentrations for A and B are then obtained from the following equations that are easily solved by the CFD software:

$$\frac{\partial \langle C_A \rangle}{\partial t} + U_j \frac{\partial \langle C_A \rangle}{\partial x_j} = \frac{\partial}{\partial x_j} \left[(D + D_T) \frac{\partial \langle C_A \rangle}{\partial x_j} \right] + \gamma_A k \langle C_A \rangle \langle C_B \rangle \quad (5.39)$$

and

$$\frac{\partial \langle C_B \rangle}{\partial t} + U_j \frac{\partial \langle C_B \rangle}{\partial x_j} = \frac{\partial}{\partial x_j} \left[(D + D_T) \frac{\partial \langle C_B \rangle}{\partial x_j} \right] + \gamma_B k \langle C_A \rangle \langle C_B \rangle. \quad (5.40)$$

5.5.2 $Da \gg 1$

The reaction rate defined in Eq. (5.3) is

$$\langle S_A \rangle = \langle S_B \rangle = -\langle k_1 C_A C_B \rangle = -k_1 (\langle C_A \rangle \langle C_B \rangle + \langle C'_A C'_B \rangle). \quad (5.41)$$

For instantaneous reactions, k_1 will have a very large value and the only way to obtain finite reaction rates is if we have

$$-\langle C'_A C'_B \rangle \approx \langle C_A \rangle \langle C_B \rangle. \quad (5.42)$$

Hence in this case the average reaction rate will be approximately zero, which is possible only if the diffusion distance shown in Fig. 5.2(a) is infinitely short. Equation (5.42) is not a closure, though. The closure for instantaneous reactions assumes that A and B cannot coexist in fluid elements. It will be shown below that it is then sufficient to calculate the mixture-fraction PDF (see Section 5.4.2) to completely describe the reacting system. Physically the rate of instantaneous reactions will peak at the centre of a mixing layer (see Figure 5.2), since this is where mixing is most intense.

Consider the instantaneous reaction between species A and B, for any combination of A and B and for any rate expression S :



Here γ_A and γ_B determine the stoichiometry and the initial conditions are given in Figure 5.9.

The instantaneous transport equations (not Reynolds averaged) for A and B read

$$\frac{\partial C_A}{\partial t} + U_j \frac{\partial C_A}{\partial x_j} = \frac{\partial}{\partial x_j} \left(D \frac{\partial C_A}{\partial x_j} \right) + \gamma_A S \quad (5.44)$$

and

$$\frac{\partial C_B}{\partial t} + U_j \frac{\partial C_B}{\partial x_j} = \frac{\partial}{\partial x_j} \left(D \frac{\partial C_B}{\partial x_j} \right) + \gamma_B S, \quad (5.45)$$

where we have assumed that A and B have the same molecular diffusivity D . Multiplying Eq. (5.44) by γ_B and Eq. (5.45) by γ_A and then subtracting Eq. (5.45) from Eq. (5.44) leads to

$$\frac{\partial(\gamma_B C_A - \gamma_A C_B)}{\partial t} + U_j \frac{\partial(\gamma_B C_A - \gamma_A C_B)}{\partial x_j} = \frac{\partial}{\partial x_j} \left(D \frac{\partial(\gamma_B C_A - \gamma_A C_B)}{\partial x_j} \right). \quad (5.46)$$

By inspection it can be seen that the constructed variable $(\gamma_B C_A - \gamma_A C_B)$ is satisfied by the same transport equation as the mixture fraction (see Eq. (5.16)) since the source term has disappeared. To be completely identical, the constructed variable must also have the same initial values as the mixture fraction. Normalization leads to a coupling between reactive scalars and the mixture fraction:

$$\xi = \frac{\gamma_B C_A - \gamma_A C_B + \gamma_A C_{B0}}{\gamma_B C_{A0} + \gamma_A C_{B0}}. \quad (5.47)$$

On substituting for $(\gamma_B C_A - \gamma_A C_B)$ from Eq. (5.46) we obtain Eq. (5.16). The inlet containing $C_A = C_{A0}$ and $C_B = 0$ gives $\xi = 1$, and for the inlet containing $C_B = C_{B0}$ and $C_A = 0$ we obtain $\xi = 0$. It is not possible to solve Eq. (5.16) for turbulent flows, but an estimation of the instantaneous mixture fractions can be done using the beta-PDF. By taking the Reynolds average in Eq. (5.28) and solving for the mixture-fraction average $\langle \xi \rangle$ and the variance in Eq. (5.29) or Eq. (5.34), we can reconstruct the beta-PDF using Eqs. (5.13)–(5.15).

For an instantaneous irreversible reaction this relation is especially favourable, since we know that A and B cannot coexist in a fluid element. So, if $C_A > 0$, we know that $C_B = 0$ and vice versa. We also know that there must be a point in mixture-fraction space where $C_A = C_B = 0$. This point is termed the stoichiometric mixture fraction ξ_s and is given by Eq. (5.47) as

$$\xi_s = \frac{\gamma_A C_{B0}}{\gamma_B C_{A0} + \gamma_A C_{B0}}. \quad (5.48)$$

On dividing Eq. (5.47) by Eq. (5.48) we can construct linear correlations between the reactive concentrations and the mixture fraction for all mixture fractions:

$$\gamma_B C_A - \gamma_A C_B = \gamma_A C_{B0} \left(\frac{\xi}{\xi_s} - 1 \right). \quad (5.49)$$

We do not know the exact value of ξ , but we can estimate a possible distribution of ξ . In other words, the reactive concentrations are given *conditional* on the value of the mixture fraction. Since these concentrations are constructed in mixture-fraction space, we use the sample-space variable η for ξ .

For $\eta \leq \xi_s$, $C_A(\eta) = 0$ and

$$C_B(\eta) = C_{B0} \left(1 - \frac{\eta}{\xi_s} \right). \quad (5.50)$$

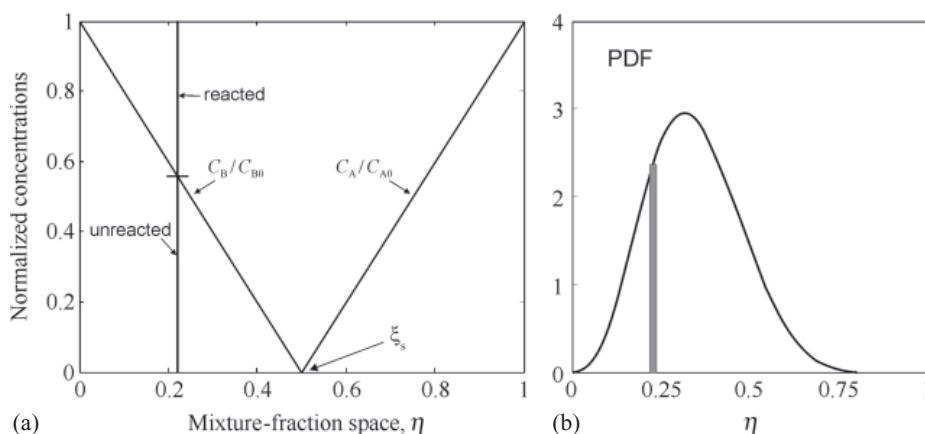


Figure 5.10 A schematic representation of the concentrations of reactive species in mixture-fraction space. The reaction between A and B is instantaneous.

For $\eta \geq \xi_s$, $C_B(\eta) = 0$ and

$$C_A(\eta) = C_{B0} \frac{\gamma_A}{\gamma_B} \left(\frac{\eta}{\xi_s} - 1 \right). \quad (5.51)$$

The concentrations of the reactive species are shown schematically in Figure 5.10(a). The total amount of A and B can then be calculated if we know the mixture-fraction distribution $\varphi(\eta)$ in the computational cell shown in Figure 5.10(b). The average concentration in the cell is the integration of the concentration at a given mixture fraction η times the frequency of the appearance of that mixture fraction, i.e. the PDF $\varphi(\eta)$. The mean concentrations can easily be calculated from Eqs. (5.50) and (5.51) weighted by the probability of finding that mixture fraction estimated from the presumed PDF of the mixture fraction:

$$\langle C_A \rangle = \int_0^1 C_A(\eta) \varphi(\eta) d\eta = C_{B0} \frac{\gamma_A}{\gamma_B} \int_{\xi_s}^1 \left[\frac{\eta}{\xi_s} - 1 \right] \varphi(\eta) d\eta \quad (5.52)$$

and

$$\langle C_B \rangle = \int_0^1 C_B(\eta) \varphi(\eta) d\eta = C_{B0} \int_0^{\xi_s} \left[1 - \frac{\eta}{\xi_s} \right] \varphi(\eta) d\eta. \quad (5.53)$$

The only term that needs to be modelled in Eqs. (5.52) and (5.53) is the mixture-fraction PDF $\varphi(\eta)$, which can be closed with, for example, the beta-PDF (see Section 5.4.2). Hence, for instantaneous reactions there is no need to calculate a mean reaction rate explicitly and there is no need for transport equations of the reactive species. For instantaneous reactions ‘mixed is reacted’ is valid, and only the fraction not mixed need be calculated. The progress of the reaction is simply obtained by calculating the average concentrations $\langle C_A \rangle$ and $\langle C_B \rangle$ along the reactor. It is important to realize that

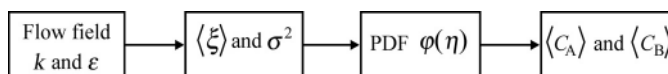


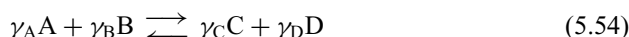
Figure 5.11 The implementation strategy for instantaneous reactions.

the expressions in Eqs. (5.50) and (5.51) follows from the instantaneous-reaction rate assumption that A and B cannot coexist in fluid elements.

Figure 5.11 shows the computational procedure to simulate the average concentration of A and B. First, the flow field is simulated using standard turbulence models. The PDF is obtained from simulation of the average mixture fraction and variance, and finally the average concentrations are obtained from integration of Eqs. (5.52) and (5.53).

In many fast reactions thermodynamics limits the conversion, but these reactions can also be simulated using the PDF method. The only restrictions are that there is no kinetic limitation and that the concentrations of reactants and products can be calculated as functions of the mean mixture fraction $\langle \xi \rangle$ and the variance σ^2 . For an isothermal or adiabatic reaction it is possible to calculate the chemical composition and temperature corresponding to the minimum Gibbs energy for all mean mixture fractions and variances. These calculations will require large computational power if they are done in each iteration, but, since the calculations depend only on the mean mixture fraction, the variance and the inlet conditions, it is possible to do the calculations in advance and store them in a look-up table.

The look-up table can be constructed by assuming an equilibrium reaction written as



with the reaction rate

$$S = k^+ C_A C_B - k^- C_C C_D, \quad (5.55)$$

where k^+ and k^- are the forward and backward reaction rate constants, respectively. On inserting this reaction rate into Eqs. (5.37) and (5.38) a mixture fraction can be formed by subtracting one of these two equations from the other:

$$\xi = \frac{\gamma_B C_A - \gamma_A C_B + \gamma_A C_B^0}{\gamma_B C_A^0 + \gamma_A C_B^0}. \quad (5.56)$$

We can also write transport equations for the products

$$\frac{\partial C_C}{\partial t} + U_j \frac{\partial C_C}{\partial x_j} = \frac{\partial}{\partial x_j} \left(D \frac{\partial C_C}{\partial x_j} \right) + \gamma_C S \quad (5.57)$$

and

$$\frac{\partial C_D}{\partial t} + U_j \frac{\partial C_D}{\partial x_j} = \frac{\partial}{\partial x_j} \left(D \frac{\partial C_D}{\partial x_j} \right) + \gamma_D S. \quad (5.58)$$

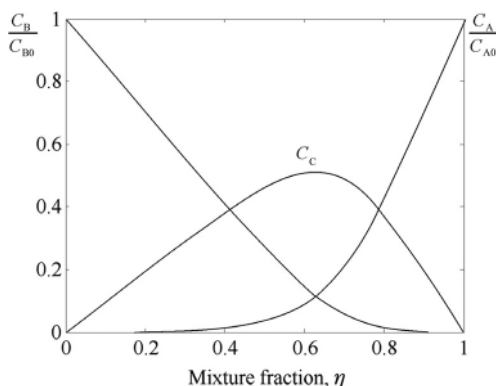


Figure 5.12 Concentrations as functions of the mixture fraction for an equilibrium reaction assuming that $C_{B0} = 2C_{A0}$.

After multiplying by stoichiometric coefficients and adding Eqs. (5.37) and (5.57), we obtain

$$\frac{\partial(\gamma_C C_A + \gamma_A C_C)}{\partial t} + U_j \frac{\partial(\gamma_C C_A + \gamma_A C_C)}{\partial x_j} = \frac{\partial}{\partial x_j} \left(D \frac{\partial(\gamma_C C_A + \gamma_A C_C)}{\partial x_j} \right). \quad (5.59)$$

On defining the mixture fraction

$$\xi = \frac{\gamma_C C_A + \gamma_A C_C}{\gamma_C C_A^0}, \quad (5.60)$$

we obtain Eq. (5.16). Since the mixture fractions formulated with Eq. (5.56) and Eq. (5.60) are identical and have the same boundary conditions, $\xi = 1$ for $C_A = C_{A0}$ and $\xi = 0$ for $C_B = C_{B0}$, they have the same solution and hence

$$\xi = \frac{\gamma_C C_A + \gamma_A C_C}{\gamma_C C_A^0} = \frac{\gamma_B C_A - \gamma_A C_B + \gamma_A C_B^0}{\gamma_B C_A^0 + \gamma_A C_B^0} \quad (5.61)$$

everywhere. For an equilibrium reaction the equilibrium balance

$$\frac{C_C^{\gamma_C} C_D^{\gamma_D}}{C_A^{\gamma_A} C_B^{\gamma_B}} = K(T) \quad (5.62)$$

must be fulfilled and the equilibrium constant is obtained from the thermodynamics:

$$K(T) = e^{\Delta S/R} e^{-\Delta H/(RT)} = e^{-\Delta G/(RT)}, \quad (5.63)$$

where ΔS is the entropy, ΔH is the enthalpy and ΔG is the Gibbs free energy for the reaction. For an adiabatic reaction, the temperature will depend on the inlet temperature and the heat of reaction:

$$T = T_1 + (T_2 - T_1)\xi + \frac{(-\Delta H)C_C}{\gamma_C \rho C_p}, \quad (5.64)$$

where T_1 is the temperature at $\xi = 0$ and T_2 is that at $\xi = 1$. Here it is assumed that the heat capacity is equal for each compound and also constant over the temperature range. The four equations (5.61)–(5.64) contain four unknowns. Hence all the concentrations and the temperature can be calculated as a function of the mixture fraction. Figure 5.12

shows how C_A , C_B and C_C vary with the mixture fraction for a typical equilibrium reaction. For non-adiabatic reactions, the heat loss must be integrated along the reaction path.

The average concentration and temperature are obtained by integrating the instantaneous variations shown in Figure 5.12 using the PDF $\varphi(\eta)$:

$$\langle C_A \rangle = \int_0^1 C_A(\eta) \varphi(\eta) d\eta. \quad (5.65)$$

The PDF is obtained from the simulated mean mixture fraction $\langle \xi \rangle$ and variance σ^2 shown in Figure 5.10(b) using the beta-PDF. The data in Figure 5.12 are obtained from the inlet conditions and thermodynamics, and the average concentrations are functions only of the mean mixture fraction $\langle \xi \rangle$ and variance σ^2 . Consequently, it is possible to pre-calculate average concentrations and temperature in a 2D look-up table. This method also allow predictions of radical species' concentrations and dissociation effects at high temperature without knowing the reaction rate, since an equilibrium condition is assumed. The cost of doing these predictions comes directly from the cost of generating a more advanced look-up table. An important limitation with excluding the kinetics is that we cannot predict ignition or extinction of reactions in combustion systems. If these phenomena are of interest, there is no way around the problem and the kinetics must be included in the simulations.

The assumption that there are no kinetic limitations and that the reaction is determined only by thermodynamics is very important. According to the equilibrium model methane can burn at room temperature. Another common problem is when the equilibrium changes very much with temperature, e.g. NO is formed from oxidation of nitrogen above 1500 K and reaches high concentrations in internal combustion engines above 2000 K. The equilibrium model will predict a reversible reaction back to nitrogen and oxygen during the fast cooling due to expansion in the cylinder. In reality this will not happen, since the reaction rate for decomposition of NO is very slow below 2000 K. It is recommended that nitrogen oxides should not be included in the equilibrium calculations if the temperature is below 2000 K. However, formation of nitrogen oxides can often be added as a homogeneous reaction since nitrogen and oxygen are already premixed in the air.

Figure 5.13 shows the different steps in modelling the oxidation of methane in air. First the look-up table is calculated. In Figures 5.13(c) and (f) the mole fraction of methane and temperature are visualized, but a look-up table will be calculated for all compounds that you selected, e.g. CO₂, CO, H₂O, H, CH etc. Note that the variable ξ ranges from 0 to 1 and σ^2 ranges from 0 to 0.25, which is the theoretical maximal variance of unmixed reactants. In the second step the flow, mean mixture fraction and variance are simulated. The temperature and composition can then be found in the look-up tables to obtain the right properties of the fluid. The mean mixture fraction, variance, methane mole fraction and temperature are shown in Figures 5.13(c)–(f). Note that the conserved scalar disappears due to dilution whereas the reactant disappears due to combustion.

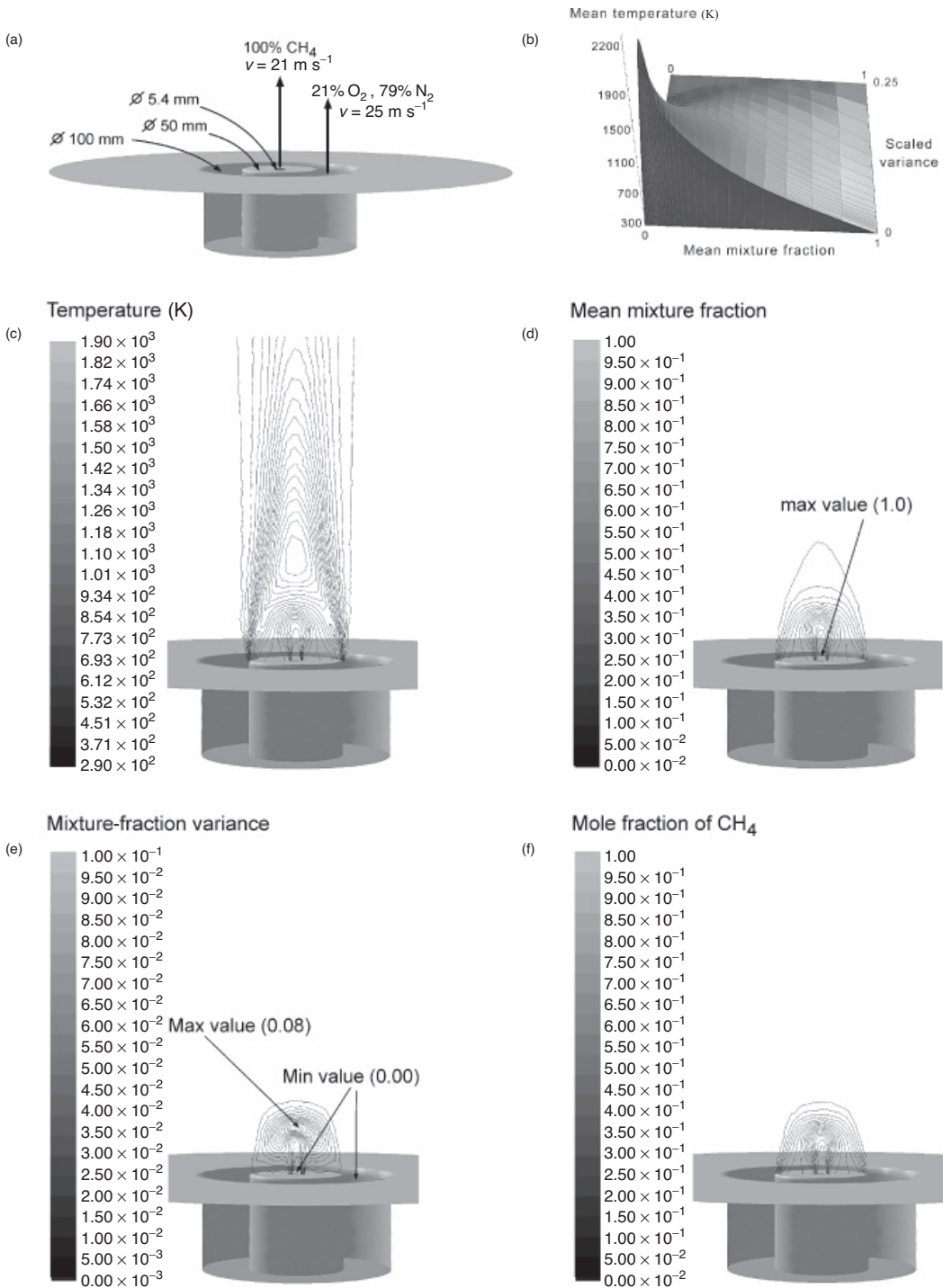


Figure 5.13 Simulation of adiabatic oxidation of methane in air: (a) configuration, (b) look-up table, (c) temperature, (d) mean mixture fraction, (e) variance and (f) mole fraction of CH_4 .

It is also possible to use such methods for non-adiabatic reactions. The compositions and temperatures in the look-up tables will then be functions of energy loss or gain also. During the iterations the energy loss or gain is estimated, which allows convection and radiation from the flame to be included in the simulations.

As mentioned before, the PDF methods have been developed only for two distinct inlet streams. For more complicated systems the theories break down and simpler models must be employed.

5.5.3 $Da \approx 1$

For intermediate Damköhler numbers A and B can coexist, and this case is by far the most difficult to close. The very simplest models which are able to give reasonably good a-priori predictions use a reaction-progress variable in conjunction with the presumed PDF of a mixture fraction. The reaction-progress variable models are similar in form to the solution presented for instantaneous reactions in Section 5.5.2. The only significant difference is that a transport equation needs to be solved for the reaction-progress variable, which in turn requires the explicit calculation of the average reaction rate. Owing to the mathematical complexity of these models, we will in this section present only one such solution for a simple reaction scheme. For a complete review of today's state of the art, the reader is referred to [15].

To be able to predict mean concentrations with a presumed PDF method, the instantaneous concentrations of the reactive species need to be known or closed subject to the mixture fraction. The instantaneous concentration subject to the mixture fraction is usually referred to as a conditional average. For instantaneous reactions the conditional concentrations have been shown to be linear in mixture-fraction space and hence closed (see Eqs. (5.50) and (5.51)). For intermediate Da , the assumption leading to Eqs. (5.50) and (5.51) does not hold and other relationships must be found. Baldyga and Bourne [14] described a model that uses piecewise linear interpolation between the extreme limits of instantaneous ($k_1 = \infty$) and slow ($k_1 = 0$) chemistry to obtain closure. Here we present this model, again for the simplest case of one fast, but irreversible, reaction as illustrated in Eq. (5.43). It is possible, though, to extend the model to more complex reaction systems.

As has already been stated, the instantaneous rate assumption fails for intermediate Da , so it is necessary to find alternative closures for Eqs. (5.50) and (5.51). The interpolation model exploits the fact that the conditional concentrations have to fall within the extremes of instantaneous and slow, for which the solutions are known. Hence the conditional concentration of A is limited according to

$$\frac{C_A^0}{C_{A0}} \geq \frac{C_A}{C_{A0}} \geq \frac{C_A^\infty}{C_{A0}} \Rightarrow \eta \geq \frac{C_A}{C_{A0}} \geq (\eta_{\xi_s}^{-1} - 1) \frac{\gamma_A C_{B0}}{\gamma_B C_{A0}}, \quad (5.66)$$

whereas the conditional concentration of B is limited according to

$$\frac{C_B^0}{C_{B0}} \geq \frac{C_B}{C_{B0}} \geq \frac{C_B^\infty}{C_{B0}} \Rightarrow 1 - \eta \geq \frac{C_B}{C_{B0}} \geq 1 - \eta_{\xi_s}^{-1}. \quad (5.67)$$

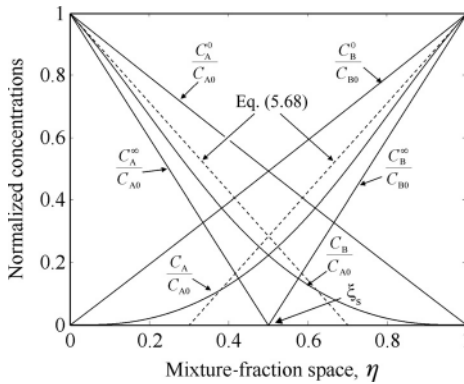


Figure 5.14 Concentrations of reactive species in mixture-fraction space. The reaction between A and B is fast.

Note that C_α^0 corresponds to pure mixing with no reaction, whereas C_α^∞ corresponds to the instantaneous reaction according to Eqs. (5.50) and (5.51). The interpolation model is now obtained by introducing a reaction progress variable Y_p ($0 \leq Y_p \leq 1$), such that the conditional concentrations are found as

$$\frac{C_\alpha}{C_{\alpha 0}} = \frac{C_\alpha^0}{C_{\alpha 0}} Y_p + \frac{C_\alpha^\infty}{C_{\alpha 0}} (1 - Y_p), \quad \text{for } \alpha = A \text{ or } B, \quad (5.68)$$

corresponding to the dotted lines in Figure 5.14. Hence the instantaneous limit is obtained for $Y_p = 0$, whereas the no-reaction limit is obtained for $Y_p = 1$. Equation (5.68) replaces Eqs. (5.50) and (5.51) in the interpolation model. However, Eq. (5.68) is still not closed due to Y_p . The closure for the reaction-progress variable reads

$$Y_p = \frac{\langle C_\alpha \rangle - \langle C_\alpha^\infty \rangle}{\langle C_\alpha^0 \rangle - \langle C_\alpha^\infty \rangle}, \quad \text{for } \alpha = A \text{ or } B. \quad (5.69)$$

The terms in angle brackets are averages computed straightforwardly as e.g.

$$\langle C_\alpha^\infty \rangle = \int_0^1 C_\alpha^\infty(\eta) \varphi(\eta) d\eta. \quad (5.70)$$

Note that Y_p is computed for just one of the species A and B, since, given either, the other can be found through Eq. (5.47). Naturally, one reaction-progress variable suffices to describe one reaction. To close Eq. (5.70) a separate transport equation for $\langle C_\alpha \rangle$ is also required:

$$\frac{\partial \langle C_\alpha \rangle}{\partial t} + \langle U_j \rangle \frac{\partial \langle C_\alpha \rangle}{\partial x_j} = \frac{\partial}{\partial x_j} \left(D_T \frac{\partial \langle C_\alpha \rangle}{\partial x_j} \right) - \gamma_\alpha k_1 \langle C_A C_B \rangle. \quad (5.71)$$

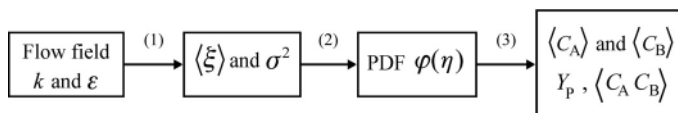


Figure 5.15 An implementation strategy for the interpolation model.

For the current purpose α can be either A or B. The average reaction rate can be computed as

$$k_1 \langle C_A C_B \rangle = k_1 \int_0^1 C_A(\eta) C_B(\eta) \varphi(\eta) d\eta. \quad (5.72)$$

where $C_A(\eta)$ is computed from Eq. (5.68) and $C_B(\eta)$ can be computed from Eq. (5.47) with $\xi = \eta$ and $\gamma_A = \gamma_B$ as

$$C_B(\eta) = C_A(\eta) + C_{B0} - \eta(C_{A0} + C_{B0}). \quad (5.73)$$

Equation (5.72) closes the problem and the interpolation model can be implemented using the strategy of Figure 5.15. First (1) the flow field needs to be computed to provide the turbulent kinetic energy and energy-dissipation rates. These parameters are then used for calculating the mean and variance of a mixture fraction using e.g. the TMM model (2) that further can be used to close the mixture fraction PDF from e.g. Eqs (5.13)–(5.15). With the PDF we can (3) compute the average reaction rate that closes the transport equation for the average reactive species.

Any model can be used for steps (1) and (2) in Figure 5.15 as long as the mixture-fraction PDF is delivered to the final step. The final step requires solution of Eq. (5.71) using Eqs. (5.47), (5.68)–(5.70) and (5.72). The average concentration in the computational cell is iterated. An initial guess of $\langle C_A \rangle$ gives the progress variable in Eq. (5.69) that is used for calculating the reaction rate in Eq. (5.72). This reaction rate is then used in solving Eq. (5.71), which produces a new value of $\langle C_A \rangle$. Note that there is only one more transport equation that needs to be solved in the CFD problem. All the remaining equations are algebraic and must be solved for in user-defined functions to provide the reaction rate as input for the transported species.

A more general procedure for implementing reaction-progress variables that can be more easily extended to multiple reactions has been described by Fox [15].

The state of the art for presumed PDF methods is the conditional moment closure that actually solves transport equations for the conditional concentrations in mixture-fraction space, instead of relying on the linear interpolations. The conditional moment closure has been applied both to combustion and to mixing-sensitive liquid reactions. One major disadvantage of the conditional moment closure is that the governing transport equations are five-dimensional (three spatial, one time and one mixture-fraction space) and thus computationally demanding. The large-dimensionality space is also one of the major problems of today's state of the art in modelling of reactive mixing, the full PDF methods, which solve transport equations for the joint PDF of reactive species. In full PDF methods the dimensional space is proportional to the number of reacting species, which can be substantial.

Table 5.2 Mixing and reaction of species A and B from different initial conditions and volume fractions

Scenario (a)	
$C_A = 1$	$C_A = 0$
$C_B = 0$	$C_B = 1$
$V_A = 0.5$	$V_A = 0.5$
Scenario (b)	
$C_A = 2/3$	$C_A = 0$
$C_B = 0$	$C_B = 2$
$V_A = 3/4$	$V_B = 1/4$

5.6 Non-PDF models

The most common reaction models found in most CFD software are based on eddy-dissipation (ED) modelling and do not incorporate a mixture-fraction PDF. The idea behind ED models is that the rate of mixing limits the mean rate of reaction. In ED two rates are computed: the reaction rate based on the mean concentrations (the slow-chemistry limit) and a scalar mixing time. Since the ED model was originally developed for combustion, the mixing time has traditionally been computed with the inertial–convective τ_{IC} timescale. However, better results could probably be obtained for liquids using, for example, the mean scalar dissipation rate in the turbulent-mixer model (Eq. (5.35)) or some other model developed for high Schmidt numbers. The mean reaction rate calculated with the ED model is

$$\langle S_\alpha \rangle = \min[S_{\text{kinetic}}, S_{\text{mixing}}] = \min[S(\langle C \rangle), c_i \langle C_\alpha \rangle 1/\tau], \quad (5.74)$$

where $\langle C_\alpha \rangle$ is the limiting reactant. The rate expression means that the reaction rate cannot be faster than a constant, c_i , times the rate of mixing. In its simplest form the rate of scalar dissipation is calculated from the inertial–convective timescale $\langle N \rangle = 1/\tau \propto \varepsilon/k$. The ED model works well for slow reactions and instantaneous reactions, and is here a simple alternative to the mixture-fraction approach. It works well for certain combustion units since the combustion reaction is slow before ignition, but can be extremely fast once ignition has started. However, the ED model gives a very simplified picture of the physics and, unfortunately, for intermediate Da it is not possible to correlate the average reaction rate with the slow and instantaneous limits. Further, the model cannot predict the dependence of mixing-sensitive reactions on the initial volume fractions of the reacting flows. From experiments it is well known that the reaction rates depend very much on the initial volume fractions of the fluids and the two scenarios in Table 5.2 should lead to very different average reaction rates despite the fact that the average concentrations are equal, $\langle C_A \rangle = \langle C_B \rangle = 0.5$.

This dependence can be captured only by incorporating the structure of the mixture, which is achieved with the more advanced mixture-fraction models discussed above. The ED model can be useful for predicting trends for instantaneous reactions, and is useful if there are multiple injections, recirculation streams or other complicating factors.

The ED model is applicable for any initial configuration, which mainly accounts for its popularity in commercial software.

5.7 Summary

In this chapter we have discussed the problems specific to reactive mixing of turbulent incompressible, isothermal flows. The major emphasis has been on modelling of a conserved scalar and the use of a conserved scalar in modelling of chemical reactions, through presumed PDF methods.

Questions

- (1) What is the most important parameter to study when you are first presented with a reactive-mixing problem?
- (2) What is meant by the mixture-fraction PDF? What is a conserved scalar?
- (3) What is the physical interpretation of the mixture-fraction variance?
- (4) Explain the most important features of the turbulent-mixer model.
- (5) What is the smallest relevant length scale for turbulent mixing? What is the physical interpretation of this scale?
- (6) What is described by the Schmidt number? What is described by the turbulent Schmidt number?
- (7) Why is it difficult to solve problems in which $Da \approx 1$?